Environmental Science and Pollution Research (2018) 25:11595–11613
https://doi.org/10.1007/s11356-018-1380-0

RESEARCH ARTICLE

Improvement studies on emission and combustion characteristics of DICI engine fuelled with colloidal emulsion of diesel distillate of plastic oil, TiO_2 nanoparticles and water

Narayanan Karisathan Sundararajan[1] · Anand Ramachandran Bhagavathi Ammal[1]

Received: 13 October 2017 / Accepted: 23 January 2018 / Published online: 10 February 2018

Abstract
Experimentation was conducted on a single cylinder CI engine using processed colloidal emulsions of TiO_2 nanoparticle-water-diesel distillate of crude plastic diesel oil as test fuel. The test fuel was prepared with plastic diesel oil as the principal constituent by a novel blending technique with an aim to improve the working characteristics. The results obtained by the test fuel from the experiments were compared with that of commercial petro-diesel (CPD) fuel for same engine operating parameters. Plastic oil produced from high density polyethylene plastic waste by pyrolysis was subjected to fractional distillation for separating plastic diesel oil (PDO) that contains diesel range hydrocarbons. The blending process showed a little improvement in the field of fuel oil-water-nanometal oxide colloidal emulsion preparation due to the influence of surfactant in electrostatic stabilization, dielectric potential, and pH of the colloidal medium on the absolute value of zeta potential, a measure of colloidal stability. The engine tests with nano-emulsions of PDO showed an increase in ignition delay (23.43%), and decrease in EGT (6.05%), $BSNO_x$ (7.13%), and BSCO (28.96%) relative to PDO at rated load. Combustion curve profiles, percentage distribution of compounds, and physical and chemical properties of test fuels ascertains these results. The combustion acceleration at diffused combustion phase was evidenced in TiO_2 emulsion fuels under study.

Keywords Distillate plastic diesel oil · Emission characteristics · Colloidal emulsion · Zeta potential · Diesel engine · TiO_2 nanoparticles

Introduction

Manufacture of transportation vehicles especially of diesel engine types are increasing in the developed and countries with growing economy. According to European statistics, 15.6 million cars were sold annually before 2013, and it was less about 20% in 2013 and Global vehicle sales reached another all-time high of 81 million units (European Vehicle Market Statistics 2014). Out of Europe's sales in 2013, diesel cars account for 53%. The Europe's regulatory authority sets more and more stringent standards on emission, that is to say, Euro 6 sets emission limits that range from 68% (gasoline carbon monoxide) to 96% (diesel particulates) lower than those established under Euro 1 in 1992. NO_x limits were reduced by 68% from Euro 4 to Euro 6. According to Healthy Eating Index 2010 (Guenther et al. 2013), NO_x from the new diesel passenger cars could have serious adverse health effects like asthma onset in children, impaired lung function, cardiovascular disease, and premature death on exposed human. It also mentions about the researches regarding evaluation of tropospheric ozone formation and its ill effect on health due to diesel exhaust emissions. On performance angle, from the average vehicle engine power and average vehicle size (footprint), the average mass of the vehicles are also reducing i.e., continuation of the trend to constrict the same amount of power, or even high, from smaller-sized engines. Hence, for obvious reasons, research fraternity is striving to explore the ways and means of reducing the pollution from engine emission and increasing the performance of the diesel engines. Some of the efforts towards these aims were in use of alternate fuels,

Responsible editor: Philippe Garrigues

✉ Narayanan Karisathan Sundararajan
ksnsrirangam@yahoo.co.in

[1] Department of Mechanical Engineering, National Institute of Technology, Tiruchirappalli, Tamil Nadu 620 015, India

adopting interdisciplinary incorporations like electronic engine governing and timed injection systems, tribological improvements, altering the fuel chemistry, regenerative techniques, catalytic emission reduction, and exhaust gas recirculation. Out of these, except alteration of fuel chemistry and use of alternate fuels, all others involve techno-economic consideration. Alteration fuel chemistry involves blending the regular petro diesel as well as alternate fuels with emulsions, nano-additives, cetane improvers, oxygenates etc. Out of alternate fuels, waste plastic oil is gaining importance recently among researchers due to extensive plastic waste generation, high calorific value, easier recovery of oil yield, solution for waste disposal, and simultaneous energy recovery.

Nevertheless, adaptation of simple and cost-effective methods can easily be commercialized and reach the real world applications for the benefit of the human usage. But still, there are challenges in such alteration of fuel chemistry like, application at varying climatic conditions, induced pollution due to additives, stability of fuel upon storage, striking the balance between emission and performance, modification in engine due to mixing of additives, and negative impact on engine tribology. Out of all these challenges, induced pollution due to additives should have to be of serious concern in the interest of environment and human health. Many research works have been made and reported in water emulsions of alternate fuels particularly with crude plastic oil and its blended fuels in CI engines. Recently, Kalargaris et al. (2017) reported that diesel-plastic oil blends (60–70%) shown good results in engine performance and emissions at 80–90% engine loads. In another work (Vu et al. 2001) with emulsified waste plastic oil, with 10 and 20% by volume of water and 0.3% volume of proprietary additives shown stability and reduction of NO_x emission by 30 and 50%. Sachin Kumar et al. (2013) reported that BSFC shown increasing and decreasing trends with increase in plastic oil blend ratio and engine load, respectively. In emissions, NO_x decreased while CO increased with the increase in engine load. Kaimal and Vijayabalan (2015) reported that, at the rated load, the peak cylinder pressure, heat release, combustion duration, and ignition delay of plastic oil and its blends were higher than that of diesel. But only seldom works were found to be reported in nano-emulsions of diesel distillate of plastic pyrolysis oil.

In a recent work of Sadhik Basha and Anand 2011, the authors reported that addition of alumina nanoparticles in diesel imparted a remarkable improvement in the performance of the engine and a reduction of harmful pollutants. In another work (Sadhik Basha 2015), the author stated that addition of Alumina nanoparticles increases the brake thermal efficiency, marginal reduction in unburnt hydrocarbons, CO emissions, and a remarkable reduction in NO_x levels. In addition, he mentioned that the nanoparticles added test fuels were stable for more than 7 days. Similar trend was also reported in the investigation (Arianna et al. 2005) while using cerium oxide nanoparticles but no evidence of considerations of report regarding toxicological implications of nanoparticles. Hence, with a quest in searching for NP with less toxicity, literature survey has been made. A recent toxicological study (Shi et al. 2013) reported that pulmonary exposures of TiO_2 NPs did not cause extensive damage to the air/blood barrier; NP translocation was slow and representing less than 1% of the initial pulmonary burden at 1 week post-exposure. Further, TiO_2 combustion in coal and its desulphurization effect when blended with CaO as catalyst was reported in earlier work (Wang et al. 2008). This result implies that TiO_2 NPs helps in pollution reduction. Hence, TiO_2 can be a better candidate for blending with the fuel. However, no substantial in-depth works have been reported in attempting towards improving the stability of plastic diesel oil emulsions after blending with TiO_2 NPs for combustion purposes in CI engines. It is obvious that no single societal problem can be solved without interdisciplinary engineering help, because several factors of a problem have their own kingdom of theories to which they bound in nature. Similarly, the stability factor depends on the science behind colloidal systems. According to that, the stability of the blended fuel depends on the dispersion efficiency of the nanoparticles with the medium present in the emulsion fuel. Usually formulation of nanofluids is pivoted by the instabilities as a result of agglomeration, flocculation, and sedimentation of nanoparticles (Brunelli et al. 2013). These deficiencies are mainly due to reduced Van der Waal forces than the force of repulsion between particles. The stability characteristic of a nanosuspension is evaluated by stability indicators such as zeta potential, UV-light transmittance and absorbance, turbidity, and sedimentation rate (Adio et al. 2014). By studying the basic principles of each of the stability indicator techniques, it understood that Zeta potential technique is the simple technique which evaluates the sample in a qualitative way and influenced greatly by pH of the test medium, dielectric constant of the dispersing medium, and the ionization potential. These unique dependencies in the technique throw light that pH and dielectric constant of the medium can be the contributing factors for stability of nanosuspensions. Obviously, if the emulsion fuel consists of water (aqueous medium), it is reasonable to expect that the proper control over the pH and dielectric constant of the dispersing medium can change the dispersion stability of nanoparticles. Further on literature survey, it is found that similar effect was studied with the Al-Cu alloy nanoparticles and reported in the literature (Samal et al. 2010).

So inspired by the above facts, with an aim to establish the effects of the combustion, performance and emission characteristics of CI engine with plastic diesel oil (PDO) fuel as an alternate fuel to regular petro-diesel, a study was attempted by altering its fuel chemistry. This was pursued by developing a tailor made blending process to improve the stability of fuel

under study, i.e., PDO fuel, water, and TiO_2 blend in the form a colloidal suspension. In the first step, the pH adjusted water-TiO_2 nano-emulsion was prepared with sodium dodecyle sulphate (SDS) as anionic surfactant to improve the stability. Then, the plastic oil was blended with suitable oil to water surfactants. Finally, TiO_2-water emulsion and the plastic oil-surfactant blend were mixed to obtain the final emulsified fuel. The detailed procedure is explained in fuel blend preparation section. The investigation is further extended by subjecting the blended PDO-water emulsion initially and tried with PDO-water-TiO_2 emulsion fuels thereafter, for any improvement that could be possible by experimenting in CI engine. Further, the results were compared with that of commercial petro-diesel fuel and its emulsions to study the effect of the altered fuel chemistry on the combustion, performance, and emission characteristics.

Materials and methods

The plastic oil produced from the batch type pyrolysis process from HDPE plastic waste in the earlier work of Narayanan and Anand (2016) has been used. Anionic surfactant, in chemical grade, SDS procured from MERK Specialties private Ltd. was used as a stabilizer in the fuel blend suspension. Laboratory Grade Di-ionized water, HCL, and NAOH pallets were purchased from MERK Specialties private Ltd. Tween-80 and Span-80 surfactants were procured from LOBA Cheme private Ltd., INDIA. TiO_2 nanoparticles (Degussa P25) were procured from the Institute of Chemical Education (ICE), University of Wisconsin, USA, of size 10 to 50 nm, and the technical parameters of the nanoparticles as mentioned by the supplier have been listed in Table 1. All the chemicals were used as procured without any secondary purification.

The plastic oil was subjected to fractional distillation with the main aim of separating diesel range hydrocarbon fuel. The process consists of cascaded heating of the pyrolysis plastic oil and the generated fuel range vapors raised in the distillation column on different temperature profiles, from low boiling point to high boiling point fuel, are condensed. Petrol grade fuel collected at the temperature range was 65 to 95 °C. Diesel grade fuel collected at a temperature range was 210 to 320 °C. In distillation process, 27% diesel grade fuel was collected and rest of all other fractional fuel percentage was 73% including light gases petrol, naphtha chemical, and heavy fuel oil.

Table 1 Technical parameters of TiO_2 nanoparticles (supplier: M/s Institute of Chemical Education (ICE), University of Wisconsin, USA)

Nano particle	Degussa P25 titanium dioxide
Approximate particle size	40–50 nm
Molecular formula	TiO_2
Molecular weight	79.866 g/mol
Rutile: anatase	85:15
Surface area	> 30 m^2/g

Fuel blend preparation

As described in section 1, the stability of a colloidal suspension is important to be considered while using them in reality. Stability of the most dispersed systems is low, in spite of their high degree of initial dispersion. In a suspension, particles that are solid in state show an affinity to aggregate and subsequent sedimentation. According to DLVO theory, the stability of a colloidal system is determined by the sum of the van der Waals attractive and electrical double layer repulsive forces that exist between particles as they approach each other due to the Brownian motion they are undergoing. This theory proposes that an energy barrier resulting from the repulsive force prevents two particles approaching one another and adhering together.

There are two fundamental mechanisms that influence the dispersion stability. One is steric stabilization, and other is the electrostatic or charge stabilization. Out of which, electrostatic or charge stabilization has the benefit of stabilizing a system by simply altering the concentration of ions in the system, which was adopted in this work. The charge stabilization is a potentially reversible process and is inexpensive. This can be made by adding surfactant ions which were adsorbed on the surface of a particle leading to a positively charged surface, in the case of cationic surfactants and in the case of anionic surfactants, to a negatively charged surface. So, the resultant charge at the particle surface influences the distribution of ions in the surrounding interfacial region, thereby increasing the concentration of counter ions i.e., ions of opposite charge to that of the particle, in the close vicinity to the surface. This causes an electrical double layer to exist around each particle. The phenomenon of formation of zeta potential over the TiO_2 NP is depicted in Fig. 1. One is an inner region (Stern layer) where the ions are strongly bound and an outer (diffuse) region where they are less firmly associated. Within the diffuse layer, there is an imaginary boundary inside which the ions and particles form a stable entity. When a particle mobilizes, ions within the boundary also move. Those ions beyond the boundary stay with the bulk dispersant. The potential at this boundary, which is referred as the surface of hydrodynamic shear, is called as the zeta potential. The magnitude of the zeta potential gives an indication of the potential stability of the colloidal system. If all the nanoparticles in suspension have a large negative or positive zeta potential, then they will tend to repel each other, and there will be no tendency for the particles to come nearer to each other. Based on this DVLO theory and

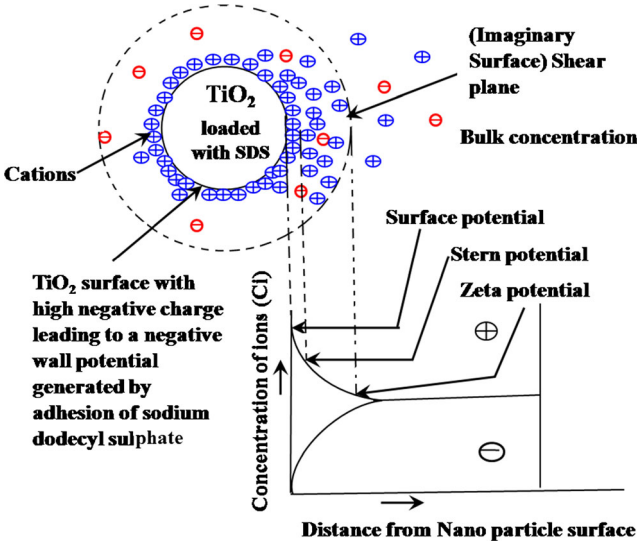

Fig. 1 Schematic representation of Zeta potential over TiO_2 particle surface

wide literature survey, a novel technique has been devised and experimented.

Initially fuel-water emulsion blends were prepared with 5% by volume of de-ionized water and 2% by volume of water to oil surfactants (SPAN 80 (HLB ratio 4.5) and TWEEN 80 (HLB ratio 14.5)) as ingredients. The surfactants each with the calculated volume obtained using Eq. 2.1 (Selim and Ghannam 2007) was separately agitated by magnetic stirring to get the expected hydrophilic–lipophilic balance (HLB) ratio of 10, as reported as the optimum value for better emulsion stability in an earlier work (Sadhik Basha and Anand 2014) and kept aside. In this equation, H_A, H_B, W_A, and W_B denote the HLB values and weights of the two surfactants, Span80 and Tween80, respectively. Then, the base fuels PDO, commercial petro-diesel (CPD), and the mixed surfactants were blended by magnetic stirring followed by ultrasonication for 30 and 15 min, respectively. Then, the mixture of surfactant and base fuels were blended with de-ionized water at the rate of 10 ml/min with the help of burette. The resulting blends are designated as PDO 2S 5 W and CPD 2S 5 W, respectively. Further, six fuel emulsion blends designated as PDO 2S 5W 20TiO_2, PDO 2S 5W 40TiO_2, PDO 2S 5W 60TiO_2, CPD 2S 5W 20TiO_2, CPD 2S 5W 40TiO_2, and CPD 2S 5W 60TiO_2 (with required amount of PDO and CPD as their base fuel respectively) were prepared in three phases. They constitute 2% by volume of water to oil surfactants, 5% by volume of pH adjusted water, and TiO_2 NPs at the loading rates of 20, 40, and 60 ppm, respectively. Primarily, the significant parameters responsible for colloidal dispersion stability of nanoparticles in emulsions have been explored for the preparation of the plastic oil-water-TiO_2 nanoparticle emulsion fuel. It is found from the literature that pH of medium, type of surfactants, concentration of surfactants (Chibowski et al. 2007) and HLB ratios of the surfactants, and dielectric constants of the dispersant and medium are the contributing factors in sustaining the dispersion stability of the colloidal suspension. In this procedure, the pH of water and loading rate of SDS reported from the earlier work (Xian-Ju et al. 2011), as optimum values in TiO_2-water nanosuspension, was followed to obtain good stability of emulsion fuel blends. In the first phase, de-ionized water was adjusted to ~13 pH by adding calculated molar proportion of pH adjustment reagent (NaOH).Then, 5% (*v*/*v*) of the pH adjusted de-ionized water, to that of the test fuel, was taken and 0.14% mass fraction of the anionic surfactant (SDS), to that of the pH adjusted water, was added to it and subjected to magnetic stirring and ultrasonication for 30 and 15 min, respectively. Then, TiO_2 nanoparticles at a loading rate of 20 ppm were added to the prepared solution with severe magnetic stirring and ultrasonication. Similarly, nanosuspensions of 40 and 60 ppm were prepared.

In the second phase, 2% (by *v*/*v*) of the mixed surfactants as prepared for H_2O-base fuel emulsion was blended with plastic diesel oil (pH ~ 6.3) of required quantity by magnetic stirring and subsequent ultrasonication for 30 and 20 min, respectively. During the third phase, the prepared pH adjusted water-TiO_2 emulsion was added to the plastic oil-surfactant emulsion by means of a burette at a rate of 20 mL/min with magnetic stirring for about 30 min and subsequent ultrasonication for 10 min. Thus, the resulting colloidal suspension obtained had a creamy pale yellowish color. Similarly, emulsion fuel with the TiO_2 loading rates of 40 and 60 ppm were prepared and kept separately for further analyses and experimentation. Three sets of sample emulsions were prepared and tested for ensuring the consistency. The results were found within 2% variation. Table 2 represents the details of emulsion fuels and their proportions, and Table 3 represents the zeta potential and pH values of the prepared emulsions. The blending process has been schematically represented in Fig. 2.

$$\mathrm{HLB_{AB}} = \left\{(H_A{}^{*}W_A) + (H_B{}^{*}W_B)\right\}/(W_A + W_B)\Big\} \qquad (2.1)$$

Characterization and property analyses of base fuels and their emulsions

The physicochemical properties of distilled PDO, CPD, and their emulsion fuels which are of prime importance for their suitability to use as fuel in C.I. engine such as density, viscosity, net calorific value, and cetane number were tested as per the relevant ASTM standards and presented in Table 4. To recognize the total compounds present in plastic diesel oil, GC-MS analysis was performed. The instrument, Perkin Elmer, model, Clarus 500 with Turbo mass with Elite-5MS capillary column (length, 30 m; internal diameter, 250 μm), and split inlet type injector were used. Oven Program was set at 40 °C (10 min) at 7 °C/min to 200 °C

Table 2 Technical details of colloidal emulsion fuels under study

Emulsion fuels under study	TiO_2 (ppm)	H_2O % by volume	pH adjusted H_2O % by volume	Base fuel % by volume	Surfactants		
					SDS (% by mass fraction to that of pH-adjusted H_2O)	Tween 80 (% by volume)	Span 80 (% by volume)
CPD	–	–	–	100	–	–	–
PD	–	–	–	100	–	–	–
CPD 2S 5W	–	5	–	93 (CPD)	–	1	1
PDO 2S 5W		5	–	93 (PDO)	–	1	1
CPD 2S 5W 20TiO_2	20	–	5	93 (CPD)	0.14	1	1
CPD 2S 5W 40TiO_2	40	–	5	93 (CPD)	0.14	1	1
CPD 2S 5W 60TiO_2	60	–	5	93 (CPD)	0.14	1	1
PDO 2S 5W 20TiO_2	20	–	5	93 (PDO)	0.14	1	1
PDO 2S 5W 40TiO_2	40	–	5	93 (PDO)	0.14	1	1
PDO 2S 5W 60TiO_2	60	–	5	93 (PDO)	0.14	1	1

(5 min) at 8 °C/min to 250 °C (3 min); vaporizing temperature of injector = 250 °C with split ratio of 1:10. Mass spectrometer instrument used electron impact ionization technique with 70 eV energy. A sample of 1.0 μL was injected, and the library model NIST 2005 was referred with. The obtained spectrum has been shown in Fig. 3, and the results are summarized and given in Table 5. The stability analysis was determined by Zeta Potential Analyzer, Zetasizer Ver. 7.11 of Malvern make (System settings = temperature 25 °C; zeta runs 73; count rate (kcps) 381; measurement position 2 mm; attenuator 7). The results of zeta potential measurements of pH adjusted water-TiO_2 emulsions and TiO_2-blended colloidal test fuels are given in Table 3.

Experiment on combustion in CI engine

Experiments on engine were performed on a single cylinder four stroke air-cooled compression ignition engine utilized by Narayanan and Anand (2016). The engine specifications and operating parameters adopted in this study are listed in Table 6. The technical specifications of the engine were supplied by the engine manufacturer (M/s Kirloskar Oil Engines Limited, INDIA). The engine experimental setup consisted of a four stroke DICI engine, AC alternator (loading device), fuel supply systems, and an emission analyzer. The cylinder pressure was measured using a Kistler 6613CA piezoelectric pressure transducer with corresponding data acquisition systems and charge amplifier. The pressure pulses were recorded for every 0.1 crank angle degree, and the data were the collective average of 50 consecutive engine cycles. Exhaust gaseous emissions were measured by calibrated AVL Di GAS 444 analyzer, chemiluminescent detector (CLD) for NO_x, flame ionization detector (FID) analyzer for UHC, non-dispersive infrared (NDIR) analyzer for CO, CO_2 measurements. A calibrated k-type chrome-alumel thermocouple was used to measure the exhaust gas temperature. Smoke opacity is measured by a part-flow smoke opacity meter (AVL Dismoke 437).

Table 3 Results of Zeta potential values for water-TiO_2 nano-emulsions and test fuels obtained by characterization

Medium	pH	Zeta potential (mV)
pH-adjusted water-20TiO_2 nano-emulsion	13.00	− 60.25
pH-adjusted water-40TiO_2 nano-emulsion	12.89	− 55.51
pH adjusted Water-60TiO_2 nano-emulsion	12.98	− 51.89
CPD 2S 5W 20TiO_2	8.58	− 29.58
CPD 2S 5W 40TiO_2	8. 40	− 31.81
CPD 2S 5W 60TiO_2	8.12	− 16.4
PDO 2S 5W 20TiO_2	8.90	− 30.68
PDO 2S 5W 40TiO_2	8.71	− 34.09
PDO 2S 5W 60TiO_2	8.10	− 30.10

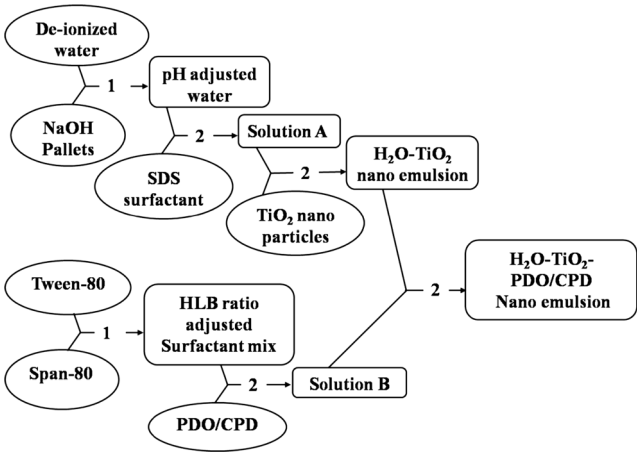

Fig. 2 Schematic representation of blending process of water-TiO_2 nanosuspension with base fuel. 1 magnetic stirring, 2 magnetic stirring followed by ultrasonication. SDS sodium dodecyle sulphate, PDO plastic diesel oil, CPD commercial petro-diesel

The engine was started with commercial petro-diesel as fuel and warmed up until the lub oil temperature was stabilized. Then, the fuel consumption, cylinder pressure, and exhaust emissions (such as NO_x, HC, CO) and smoke opacity were measured. Initially, water emulsions of base fuels (PDO 2S 5W, CPD 2S 2W) were employed, and the data were recorded. Similar experiments were repeated for the six test fuels namely PDO 2S 5W 20 TiO_2, PDO 2S 5W 40 TiO_2, PDO 2S 5W 60 TiO_2, CPD 2S 5W 20 TiO_2, CPD 2S 5W 40 TiO_2, and CPD 2S 5W 60 TiO_2. The accuracy of the measured values in emissions had been taken care by the built-in system of the gas analyzer that calibrates the gas analyzer before each measurement with that of reference gas. All the experiments were conducted at constant speed of 1500 (± 10) rpm at eight different loads of increasing trend at a constant injection timing of 26°CA bTDC. Experiments on each test fuel were repeated thrice, and the averages of the measurements were recorded at steady state and identical conditions, and the consistency of all the results were found to be within 2%.

Error analysis

The results and subsequent corollary of the experiments may be prejudiced due to errors in usage of instruments, their condition and calibration, ambient, reading, observation, and test sequence. Hence, the accuracies of the experiment results were validated by conducting error analysis on measured and calculated values using the method followed in the earlier work (Narayanan and Anand 2016). The percentage uncertainty of brake thermal efficiency was calculated from percentage uncertainties of the instruments, and the results are given in Table 7.

Results and discussion

According to the results of GC-MS analyses of plastic diesel oil, totally 120 compounds were present that mainly constitutes n-aliphatic alkanes, alkenes, cycloalkanes, alkyne, trivial amount of alcohols, and aromatic hydrocarbon. The carbon chain distribution, from GC-MS analyses, of plastic diesel oil under study has been given in Table 8. The prepared blended emulsions were kept for 3 h to attain equilibrium before subjecting to tests. Further, no phase separation among water and fuel in H_2O-base fuel emulsion up to 10 days. In TiO_2-H_2O-base fuel emulsion, no phase separation among water and fuel or settlement of TiO_2 was observed in the pale

Table 4 Physical and thermal properties of PDO, CPD, and their emulsions under study obtained by characterization

Test fuels	Density at 15 °C, g/cm^3 (ASTM D1298)	Viscosity at 40 °C, cSt (ASTM D445)	Net calorific value, MJ/kg (IS 1448 part 6 and 7)	Flash point, °C (ASTM D93)	Cetane index (ASTM D976)
PDO	0.80	4.0	42.3	48	49.1
PDO 2S 5W	0.83	5.15	40.3	60	43
PDO 2S 5W 20TiO_2	0.835	5.21	41.75	65	43.3
PDO 2S 5W 40TiO_2	0.838	5.26	41.63	65	43.8
PDO 2S 5W 60TiO_2	0.838	5.49	41.71	69	41.9
CPD	0.84	4.2	42.1	51	45.2
CPD 2S 5W	0.855	5.35	40.25	64	42.1
CPD 2S 5W 20TiO_2	0.861	5.41	41.4	66	42
CPD 2S 5W 40TiO_2	0.865	5.42	41.21	66	41.8
CPD 2S 5W 60TiO_2	0.848	5.50	41.19	67	41.1

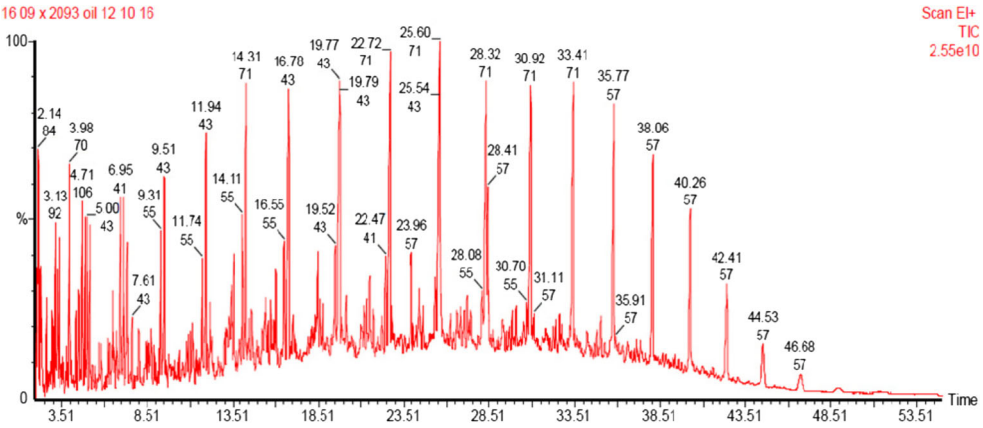

Fig. 3 GC-MS spectrum of PDO test fuel under study

yellowish creamy emulsion for 7 days. To substantiate the results, the TiO_2-blended emulsion fuels were subjected to zeta potential analyses. Out of six samples, results of PDO 2S 5W 40TiO_2 and CPD 2S 5W 60TiO_2 test samples recorded a maximum zeta potential value of − 34.09 mV and a minimum value of − 16.4 mV, respectively. The zeta potential graphs obtained are represented in Fig. 4. Since the pH of the all the test samples was found to vary from 8.10 to 8.9 because of NaOH addition, due to the basic characteristics of the nanosuspension, the number of OH^- ions in the vicinity of nanoparticles increases as the pH increases above a value of 7. Further, Fairhurst and Lee (2011) reported that, pH of the dispersion medium is responsible for the diverse rates of the corresponding ionization, association that occur in the surface functional groups as a result of the different changes in the hydration-dehydration reactions involved. Labib and Williams 1984; Fowkes et al. 1982 reported that the charge arises on the nanoparticle surface where acid-base (electron donor or acceptor) interactions occur between the particle surface and the dispersing agent, are responsible for the dispersion stability. Moreover, it was also reported by earlier researchers (Kalliola et al. 2016; Choudhary et al. 2017) that increase in pH of the polar medium of the suspension might have increased the dispersion stability. This will eventually raise the zeta potential value more than the − 30, a general dividing line in the negative side between stable and unstable suspensions. In an earlier research work (Zawrah et al. 2016), it was reported that the anionic SDS surfactant was more effective than the cationic ones. In the test fuels under study, it is found that the zeta potential values decreased from − 55.51 mV for water-TiO_2 (40 ppm loading) nano-emulsion prepared during the first phase to − 34.09 mV (PDO 2S 5W 40TiO_2) for final emulsion preparation. This might be owing to the decrease in overall dielectric constant. It is attributed to the fact that, as reported in literature (Koo and Kleinstreuer 2005), the stability increases as the dielectric constant of the nanoparticle is nearer to the dielectric constant of the dispersion medium. Since the dielectric constant of water is 80 which is nearer to the dielectric constant of TiO_2 nanoparticles (~ 60) (Löberg et al. 2013), this might be the reason for the increased value of zeta potential of the water-TiO_2 nanosuspension. After preparation of the fuel, the overall dielectric constant might have decreased because the PDO and CPD having substantial proportions of alkanes possessing a very low dielectric constant (Sen et al. 1992). Since the final dispersion medium in this work is not pure polar media (water), i.e., the partly non-aqueous medium, the charge arises will not be as strong as that would form with pure polar media. This is owing to the poor dielectric constant of alkanes (~ 2) when compared with the water (~ 80) which will hinder the degree of ionization. However, this hindering effect might have been compensated to certain extent by the presence of 5% water and appropriate amounts of surfactants, preferably anionic (SDS), as reported in earlier work (Xian-Ju et al. 2011). SDS ($C_{12}H_{25}$-OSO_3^--Na^+) is basically an anionic surfactant having amphiphilic molecules (i.e., molecules with both hydrophobic and hydrophilic regions) that constitute a hydrophobic alkyl region and a hydrophilic charged group. SDS constitutes a C_{12} H_{25} straight-chain alkyl functional group (hydrophobic tail) attached to a charged OSO_3^- group (hydrophilic head). This is represented in Fig. 5. The charged hydrophilic end of these molecules adsorb to water particles laden on TiO_2 nanoparticles, extending the hydrophobic end (Kirby 2009). So, when used as surfactant, all the hydrophilic

Table 5 Summary of results from GC-MS analysis of base test fuels obtained by characterization

Compound belonging to	Composition %	
	PDO	CPD
Alkane	69.6	67.7
Alkenes	15.9	3.2
Alkyne	2.4	–
Aromatics	8.5	21.1
Cycloalkanes	3.2	7.8
Alcohol	0.0786	–

Table 6 Technical specifications and operating parameters of engine experimental setup under study

Engine details	
Make/model	Kirloskar/TAF1
Type	Single cylinder, four stroke, naturally aspirated, air cooled, constant speed, direct injection.
Bore and stroke	87.5 × 110 mm
Length of connecting rod	220 mm
Compression ratio	17.5:1
Swept volume	661 cm^3
Combustion chamber	Open hemispherical
Nozzle	3 holes, 0.25 mm diameter
Spray cone angle	110°
Rated output and speed	4.4 kW
Injection timing	26° bTDC
Injection pressure	215 bar (21.5 MPa)
Data acquisition system	
Type	Run time, Windows XP
Specifications	12 bit, 8 channel analog-digital conversion, 12 bit channel digital-analog conversion, 4 digital input, 4 digital output, USB compatible.
Signal conditioning	Stand alone for each sensor
Pressure transducer	
Make	KISTLER
Model no.	6613CA
Measuring range	0–100 bar
Sensitivity	25 mV/bar

heads crafts a strong negative surface charge around the surface of the TiO_2 nanoparticles. This phenomenon is represented in Fig. 6. However, sedimentation of TiO_2 particles was found in all TiO_2 emulsion samples after 5 days, and still no phase separation of water and plastic oil were found. This is due to the fact that the density of TiO_2 is high when compared to the dispersant medium which will eventually cause sedimentation due to gravity. It is also observed that after mild shaking, the TiO_2 particles disperse in the medium. This could be due to the fact that though the TiO_2 particles sediment at the bottom, they were as separate entities with no force of attraction for agglomeration due to the existence of high charge potential difference imparted by the anionic surfactant between the medium and the particles.

Table 7 Estimated and calculated values of uncertainty

Sl. no	Quantity/instrument	Measuring range	Percentage uncertainty
1	AVL five gas analyzer	CO, 0–10% vol.	± 0.3
		UHC, 0–20,000 ppm	± 0.2
		CO_2, 0–20% vol.	± 0.2
		O_2, 0–22% vol.	± 0.2
		NO_x, 0–5000 ppm	± 0.2
2	AVL smoke opacity meter	0–100%	± 0.1
3	Exhaust gas temperature	0–1000 °C	± 0.1
4	Speed measuring unit	0–5000 rpm	± 0.5
5	Alternator output (brake load)	6 kW	± 0.5
6	In-cylinder gas pressure	0–100 bar	± 0.1
7	Crank angle encoder	0–360 °CA	± 0.2
8	Digital stop watch	± 0.5 s	± 0.2
9	Brake thermal efficiency	–	± 1.24

Table 8 Distribution of carbon number in PDO fuel under study obtained by characterization

Range of carbon number	Distribution (%)
C_8–C_{10}	22.35
C_{11}–C_{15}	30.15
C_{16}–C_{20}	32.32
C_{21}–C_{26}	15.09

Thus, the study reveals that, based on the difference in the dielectric constant between nanoparticle and dispersion medium, pH of the dispersion medium and the type of surfactant used as discussed above the zeta potential varies. Though the previous studies in nanoblends were reported in pure water-TiO_2 emulsions, very seldom attempts were done on water-TiO_2-aliphatic fuel emulsions. Probably, this work evidences an attempt in the little advancement towards the stability of colloidal suspension especially water-TiO_2-aliphatic fuel emulsions in line with one of the objective of this study.

Combustion characteristics

In combustion characteristics, the ignition delay of 3.2 and 4.2 °CA were recorded for PDO and CPD fuels respectively at rated load. When compared with the PDO, the reason for the delay in attaining the maximum peak pressure can be appreciated from the distribution of compounds and carbon number in CPD. Increased proportions of aliphatic compounds (alkanes and alkenes) and significantly reduced amount of aromatics were present in PDO which was found in GC-MS analyses. Aliphatic compounds possess lower ignition delay than aromatics due to their structural influence (Imdadul et al. 2015). Furthermore, the usual carbon range for CPD fuel will generally fall between C_9 and C_{24}, and the aliphatic compounds constitute 70.9%. The PDO fuel under study totally contains 87.9% aliphatic compounds, and the proportional higher carbon number distribution was C_8 to $C_{15} = 52.50\%$, and C_{18}–$C_{26} = 47.41\%$ as evidenced from GC-MS analyses. Usually 10–20 °C decrease in boiling point will be evidenced for every one carbon number reduction in alkanes (Morrison and Boyd 1982). This considerable percentage of aliphatic compounds on lower carbon number range possessing low boiling point in PDO might be the reason for the lesser ignition delay relative to CPD. An another reason for this as learnt from the literature (Hucknal 1985) is that, the availability of weaker bond strengthened alkenes (weaker C–H bonds), relative to alkanes, to tune of 15.9% might have helped to produce earlier oxygen-free radicals by hydrogen abstraction thereby reduced the chemical part of ignition delay. The CPD constituting 21.1% aromatics basically have higher density relative to aliphatic groups which could be reason for increased physical part of the ignition delay. This is also evidenced in physical property analyses (Table 5). However, the distribution of compounds and their

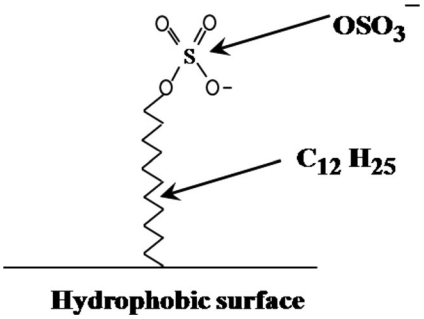

Fig. 5 The structural representation sodium dodecyle sulphate (SDS) with their two groups. 1 (OSO_3) charged group (hydrophilic head of SDS) and 2 C_{12} H_{25} (hydrophobic tail of SDS)

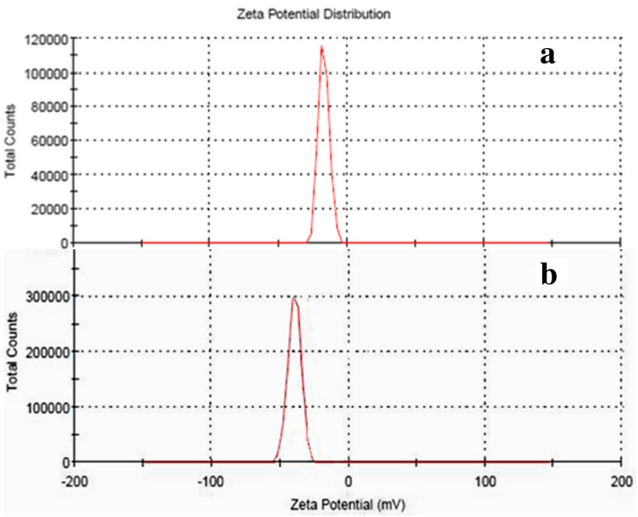

Fig. 4 Zeta potential. **a** CPD 2S 5 W 60TiO_2. **b** PDO 2S 5 W 40TiO_2

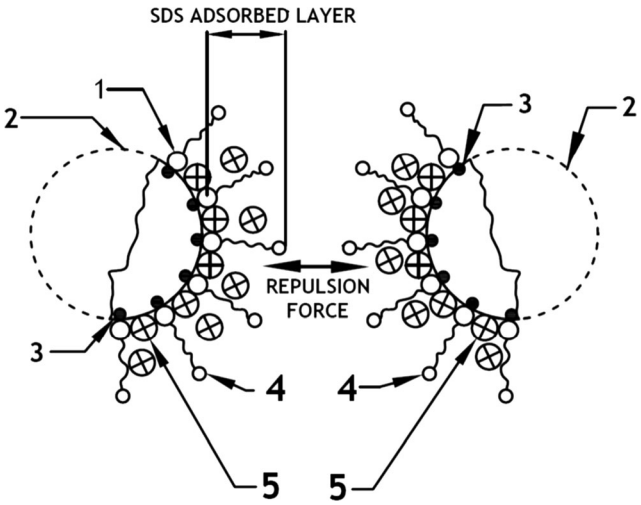

Fig. 6 The schematic representation of phenomenon of electrostatic or charge stabilization by negative charge crafting over TiO_2 nanoparticles in emulsion fuel. 1 (OSO_3) charged group (hydrophilic head of SDS); 2 TiO_2 nanoparticles; 3 H_2O particles laden over TiO_2 nanoparticles; 4 C_{12} H_{25} (hydrophobic tail of SDS); 5 attracted cations

carbon number range depends on the distillation and pyrolysis processes. In water-base fuel emulsions, an ignition delay of 4.3 and 4.9 was recorded for PDO 2S 5W and CPD 2S 5W fuels respectively at rated load. This could be due to 7.9% reduction in cetane index CPD compared to that of PDO.

When comparing water emulsions, the maximum peak pressure of 70.97 MPa was recorded for PDO 2S 5W fuel at rated load. The HRR values of 49.25 and 49.36 J/°CA were recorded for PDO and PDO 2S 5W fuels, respectively. This shows insignificant improvement in the HRR. This might be due to the poor participation of micro sized water particles in secondary explosion in combustion reaction. CPD and CPD 2S 5W recorded HRR values of 47.30 and 47.85 J/°CA respectively and peak pressure values of 68.38 and 68.16 MPa at rated load. This also shows no improvement in both HRR and maximum peak pressure. Further when studying the combustion data of nano-emulsion fuels, initial 10% of mass fractions were burnt in 2.2 and 3.2 °CA durations with PDO oil and PDO 2S 5W 60TiO_2 test fuels respectively at rated load. This is attributed to the fact that during premixed combustion phase, the combustion rate was slowed down due to the low cetane number of nano-emulsion fuel and the consequential increase in ignition delay. This is also supported by the reduced cetane number from the chemical property analyses. Finally, 80% of mass fraction burning took place in 8.9 and 11.9 °CA durations for PDO oil and PDO 2S 5W 60TiO_2 respectively at rated load. However, at loads nearing rated load, the reduction in combustion duration or increased rate of combustion at diffused combustion phase, considering the proportionate percentage mass fraction burnt during premixed combustion phase, might be due to the combustion of exposed nanosized water and fuel droplets loaded over the higher surface area of TiO_2 nanoparticles in spite of lower cetane number than PDO. This combustion acceleration might be as a result of secondary explosions of nanowater particles loaded on surface nanopores of the TiO_2 particles that releases hydroxyl radical (•OH) which is a strong one among oxygen-free radicals called "reactive oxygen species" (ROS). At elevated temperature during combustion, the reaction of an •H atom formed during the previous chain reaction with oxygen in the suction air leads to an •OH radical and to an oxygen atom, which sequentially redevelop an •OH radical by hydrogen atom abstraction from the fuel (Blocquet et al. 2010). This reaction ensures the full combustion of fuel. This might be reason behind the reducing trend in ignition delay as the load increases. The variation of ignition delay with respect to bmep has been represented in Fig. 7. The ignition delay for both CPD 2S 5W and PDO 2S 5W initially decreases with the addition of TiO_2 nanoparticles (at 20 ppm loadings), and then increases with increasing rate of TiO_2 nanoparticles (at 60 ppm loadings). The reason for this effect is explained as under. It is well established that, the ignition delay is inversely proportional to the cetane index and directly proportional to

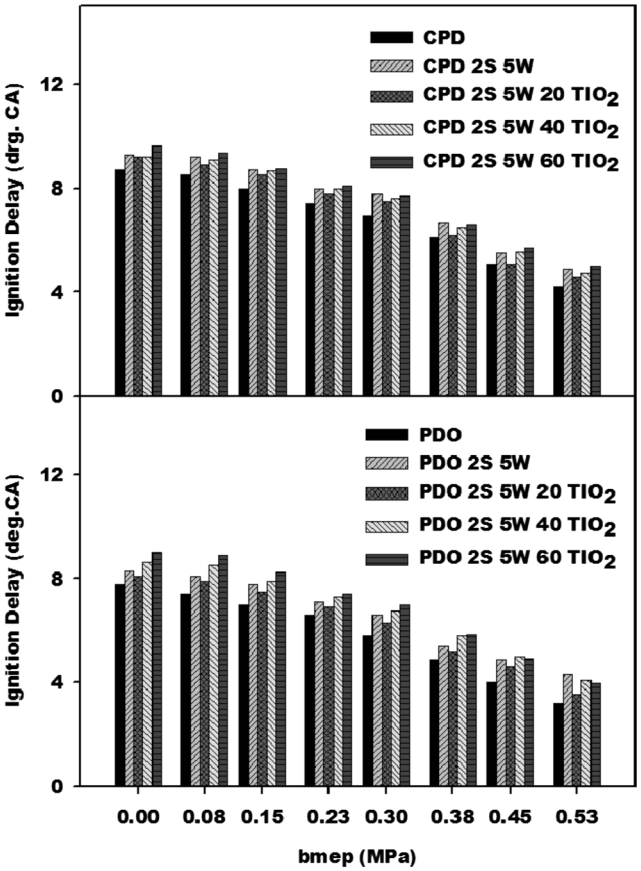

Fig. 7 Variation of ignition delay with respect to bmep for test fuels

the viscosity of the fuel. In addition, as the viscosity of the fuel increases, the fuel atomization and subsequent mixing of fuel would adversely get affected. As observed from the physico-chemical property evaluation, in case of 20 ppm loaded fuel (PDO2S 5W 20TiO_2), as a combined effect of improvement in the cetane index (0.6%) and only a marginal rise in the viscosity (1%), reduction in the ignition delay was evidenced. However, as the loading rate of nanoparticles increases to 60 ppm (PDO2S 5W 60TiO_2), a reduction in cetane index (2.5%) and rise in viscosity (6.6%) were observed in physico-chemical analyses. This synergic effect might have caused the ignition delay to increase during combustion.

Further, maximum HRR at 0.44 and 4.8 °CA aTDC and the maximum pressure rise at 4.84 and 12.7 °CA aTDC with PDO oil and PDO 2S 5W 60TiO_2 emulsion fuels respectively were recorded at rated load. This dragged HRR with PDO oil (Fig. 8) might be elucidated by the reason that the high enthalpy of vaporization of water and heat capacity of water vapor which might have participated in combustion. In TiO_2 laden emulsion fuel, accelerated HRR nearer to TDC took place, that too for a smaller crack angle sweep. Anyhow, this could be the possible rationale behind the EGT which will be beneficial in reducing other factors detrimental for the engine emissions like UHC and CO as observed in combustion and emission characteristics, respectively. PDO 2S 5W 20TiO_2 test

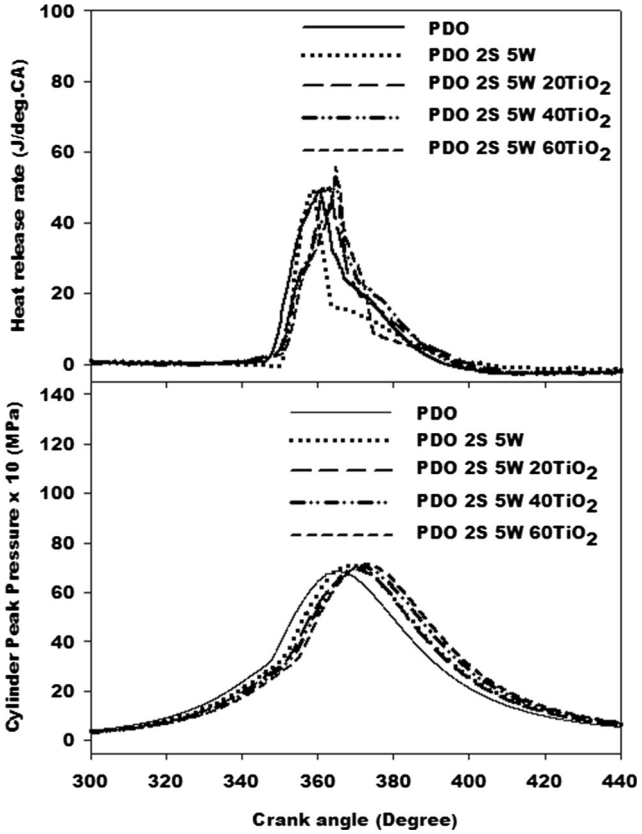

Fig. 8 Variation of H.R. rate and cylinder pressure with respect to crank angle for plastic diesel fuel-based test fuels at rated load

fuel, except an increase in ignition delay, shows insignificant change in combustion characteristics with respect to PDO. Among PDO and its emulsions, a maximum HRR of 55.79 J/°CA was recorded for PDO 2S 5W 60TiO_2 emulsion fuel. This is evidenced in the HRR curve and also that accelerated rise of HRR started sharply after TDC when comparing PDO 2S 5W 20TiO_2 especially at rated load. To demonstrate this, a combustion analysis was done with the data obtained from the recorded values during combustion, especially in diffused phase, of the test fuels and represented in Table 9. For this analysis, data of crank angle and corresponding peak HRR were taken at two positions and calculated namely (1) peak HRR crank position and (2) two crank angle degrees just before peak HRR position (arbitrarily chosen to fit the data in diffused combustion phase). This analysis throw light about the acceleration in the rate of rise of HRR/degree CA, particularly in diffused combustion phase, to a tune of 122 and 212% with the CPD 2S 5W 40TiO_2 and PDO 2S 5W 60TiO_2 respectively over their corresponding base fuels (CPD and PDO). This might be the possible indication for the accelerated HHR very nearer to the TDC position (both bTDC and aTDC) owing to the participation of TiO_2 laden water particle in secondary explosions in the case of nano-emulsion fuels. This was also evidenced from the ID of 4.75 and 3.95 °CA that were observed with CPD 2S 5W 40TiO_2 and PDO 2S 5W 60TiO_2 at rated load, respectively. This is 13.09 and 23.43% and higher than that of their respective base fuels at rated loads.

Initial 10% of mass fractions were burnt in 2.9 and 4.1 °CA durations with CPD oil and CPD 2S 5W 40TiO_2 test fuels, respectively, at rated load. This might be due to the same reasons mentioned for plastic diesel oil, but it was comparatively prolonged when compared to PDO and its emulsions due to the presence of lower percentage of alkane and considerable percentage of aromatic compounds in CPD than PDO as evidenced from the GC-MS analyses (Table 5). Since aromatics possess low cetane number relative to alkane compounds, ignition delay was increased in CPD and its emulsions. Further for CPD and CPD 2S 5W 40TiO_2, 80% of mass fraction burning took place in 9.6 and 13.2 °CA durations respectively at rated load. The reduction in combustion duration when compared to the initial fractional mass burning could be again due to the same reasons mentioned for PDO fuels. A maximum HRR at 0.88 and 6.16 °CA aTDC and the maximum pressure rise at 6.60 and 11.01 °CA aTDC with CPD oil and CPD 2S 5W 40TiO_2 emulsion fuels respectively were recorded at rated load. The emulsion CPD 2S 5W 60TiO_2 recorded a low HRR value of 41.00 J/°CA and peak pressure value of 65.81 MPa. This could be due to the poor emulsion stability, as evidenced in zeta potential analysis, and subsequent agglomeration of fuel particles which will drastically reduce the combustion reactions. The HRR curves for CPD test fuels are shown in Fig. 9. However, HRR of 49.25 J/°CA and 47.30 J/°CA were recorded for PDO and CPD fuels under study. This could be due to the marginally higher calorific value of PDO than the CPD. Though the increase in HRR is found to be advantageous with both the emulsion fuels of PDO and CPD in performance characteristics point of view such as brake thermal efficiency, a mild increase in engine noise was felt which might be due to the type of compounds present and secondary explosions of water laden TiO_2 particles in diffused combustion phase. Hence, from the combustion characteristic point of view, the optimum loading rates of TiO_2 were found to be 40 and 60 ppm with 5% water addition among CPD and PDO emulsion fuel oils under study, respectively.

Performance characteristics

The performance characteristics such as the brake thermal efficiency (BTE) and brake specific fuel consumption (BSFC) have been evaluated based on the experimentally observed data for the ten test fuels and are represented graphically with reference to bmep. The water emulsions of CPD and PDO showed a decrement of 1.29 and 1.72% in BTE at rated load than their base fuel. Blended nano-emulsion of PDO base fuel with 20 ppm TiO_2 loading shows a significant reduction of 1.43% in BTE than its base fuel. However, with

Table 9 Experimentally obtained data and arrived results of diffusion phase combustion analyses for test fuels at rated load

Test fuel	Positional importance	CA (degree)	HRR (J/°CA)	HRR/degree CA rise (slope)	% rise of HRR/degree CA increase within the base fuel and its emulsion
CPD	Instantaneo-us*	358.23	41.26	2.27	122
	Peak HRR CA position	360.88	47.30		
CPD 2S 5W $40TiO_2$	Instantaneo-us*	363.96	41.64	5.06	
	Peak HRR CA position	366.16	52.78		
PDO	Instantaneo-us*	358.23	44.77	2.02	212
	Peak HRR CA position	360.44	49.25		
PDO 2S 5W $60TiO_2$	Instantaneo-us*	362.20	39.13	6.31	
	Peak HRR CA position	364.84	55.79		

*Instantaneous position has been taken arbitrarily 2° before peak HRR CA position for analysis purpose

40 and 60 ppm TiO_2 loading in fuel shows only 0.82 and 0.06% reduction in BTE respectively at rated load than their base fuels. This result is supported by the trivial decrease in calorific value PDO emulsion fuels. In spite of the low CV, the catalytic action of the nanoparticles might have increased the combustion efficiency. Though, a little shift in bTDC angle for start of combustion is evidenced with PDO 2S 5W $60TiO_2$ due to decrease in cetane index than PDO, 4.40 CA duration aTDC has been taken for reaching maximum HRR position than that of PDO fuel. This is attributed to the fact that the TiO_2 nanoparticles having higher surface area that holds the water molecules might have involved in the secondary explosions especially more in diffused combustion phase. The nano-explosions disassociate OH-free radicals which contribute improved combustion of hydro carbons (Hasannuddin et al. 2015) and better exploitation of chemical energy. The better exploitation of energy and higher HRR are the possible reasons for the compensative recovery in thermal efficiency of PDO nano-emulsion fuels. However, increase in peak pressure owing to higher HRR during diffused combustion phase due to aforesaid reasons and subsequent recovery in BTE becomes the rationale for exercising control over BSFC of PDO 2S 5W $60TiO_2$ within a marginal increase than that of PDO. Figure 10 represents the trend of BTE among the emulsion fuels of PDO and CPD base fuels with varying bmep. Obviously, special techniques are required to get a better dispersion of the TiO_2 nanoparticles in fuel emulsion owing to their higher mass density. However, for the same injection pressure, it was found as advantageous due to the increase in gained momentum of the NPs having high mass density, after injection, will bring the fuel deep into the compressed air than the plain fuel without the nanoparticles. This might be a

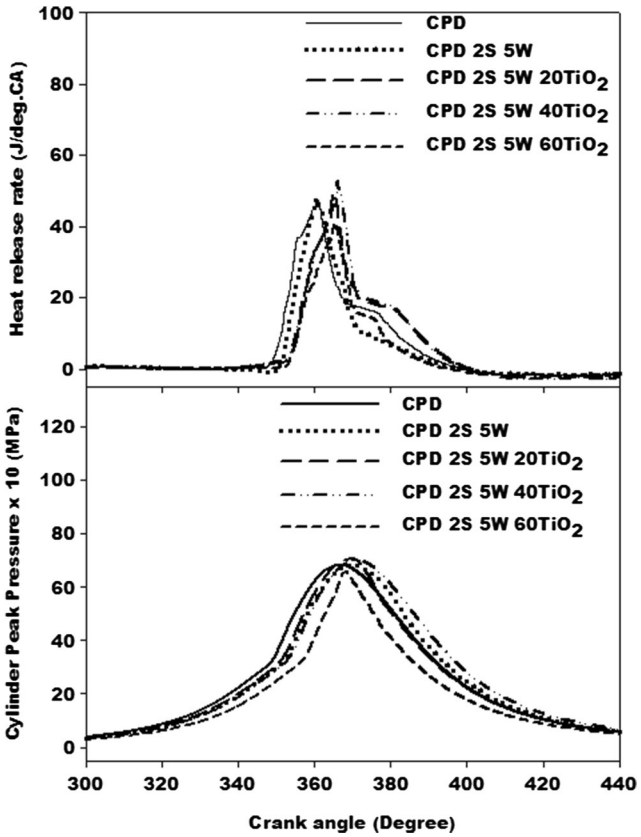

Fig. 9 Variation of H.R. rate and cylinder pressure with respect to crank angle for commercial petro fuel-based test fuels at rated load

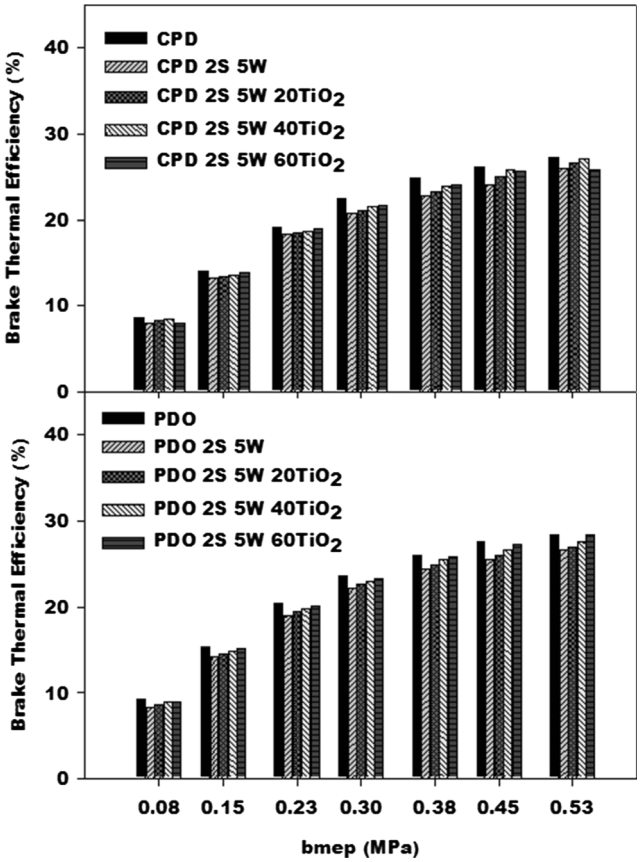

Fig. 10 Variation of BTE with respect to bmep for test fuels

possible reason for the better mixing and consequent increase in the thermal efficiency.

A reduction in the BTE (1.15%) for CPD when compared to PDO at rated load was arrived which might be due to structural influence of aromatics (Narayanan and Anand 2016) contained in CPD (21.1%) which would invariably increase the chemical part of ignition delay and consequent reduction of heat release in premixed combustion phase than that in diffused combustion phase. Brake thermal efficiency (BTE) of 26.58 and 27.17% were arrived from combustion data of CPD 2S 5W 20TiO_2 and CPD 2S 5W 40TiO_2 respectively in CI engine at rated load. This recovery in BTE might be due to the same reasons discussed for PDO fuel emulsions but with 60 ppm loading rate in CPD emulsion fuel, a lowest BTE value of all test fuels (25.87%) was arrived at rated load which might be due to the poor dispersion stability of emulsion. However, a slight increase in combustion noise was observed at peak load in PDO 2S 5W 60TiO_2 and CPD 2S 5W 40TiO_2 fuels due to the reasons discussed in combustion analyses. Hence, as a corollary, in performance characteristic point of view, the optimum loading rates of TiO_2 among the test fuels under study were found to be 40 and 60 ppm with 5% water addition for CPD and PDO fuels, respectively. Due to increase in combustion noise, and the recovery rate of BTE is low as the TiO_2 loading increases, further increase in water and TiO_2 loadings may not be advisable with existing engine operating parameters.

Figure 11 represents the trend of BSFC change between CPD, PDO, and their emulsion fuels at varying bmep. Water emulsion of PDO fuel recorded a significant increase of BSFC to a value of 19.47 g/kWh (8.08%) than its base fuel. This is due to the reduction in calorific value. An improvement was evidenced with PDO 2S 5W 60TiO_2 and CPD 2S 5W 40TiO_2 by the way of recovery in BSFC to value of 5.7 and 5.6% when compared with their water emulsion fuels. This might be due to the increase in HRR and peak pressure owing to the participation of nano-sized water particles entrapped in the nanopores of TiO_2 in spontaneous explosion at higher temperature, which cannot be expected from water-base fuel emulsion. This might have reduced the demand of fuel to maintain the same power output. However, a better recovery in BSFC was recorded with increase in loading rates of TiO_2 in PDO emulsion fuels which are low at lower loads and high as the load approaches to peak load. This recovery might be due to the synergic effect of water loaded TiO_2 nanoparticles, as discussed in combustion characteristics in detail. A decrease in BSFC (7.5%) was recorded with PDO when comparing with CPD fuel at rated load due to the marginal decrease in calorific value of CPD (Table 4). With the nano-emulsions of CPD, the same trend was observed except for CPD 2S 5W

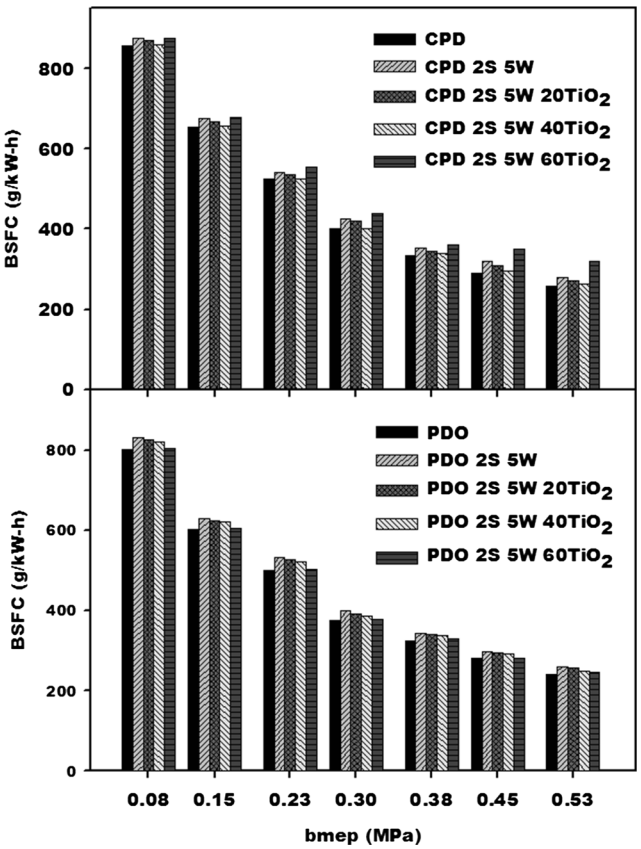

Fig. 11 Variation of BSFC with respect to bmep for test fuels

$60TiO_2$ which recorded a maximum of 320.37 g/kWh at rated load. This trend might be owing to the poor dispersion stability evidenced with CPD 2S 5 W $60TiO_2$ and the reduced calorific values relative to CPD (base fuel) to maintain the speed of the engine at their respective loads. PDO fuel records the minimum of 240.74 g/kWh at rated load. The results showed that BSFC, NOx, HC, and CO decrease, while BTE and EGT increase with the TiO_2-loaded fuels. However, while the exhaust losses increase, the primary factors for the increase of thermal efficiency are (1) improved brake power and reduced BSFC. Brake power is in turn proportional to peak pressure. (2) Engine exhaust losses are secondarily responsible. In case of TiO_2-loaded nano-emulsions, it is evident from the combustion curves (Figs. 8 and 9) that the peak pressure increases as the loading rate increases. From the experimental observations depicted in Fig. 11, it is evident that the BSFC reduces as the loading rates of TiO_2 increases. The reason for these factors is well explained earlier in this and combustion characteristics sections. Hence, the inevitable losses through engine exhaust and radiation losses which are common in all the fuels impact less or overridden by the synergic effect of peak pressure and BSFC on thermal efficiency.

Emission characteristics

Regulated emissions such as NO_x, CO, CO_2, HC, smoke, and EGT were measured for PDO, CPD, and their emulsion fuels and recorded for analyses. Out of these, it is obvious that NO_x, smoke, CO, and EGT are of main concern in the design and operating conditions of CI engines. 8.44% reduction in NO_x emission was recorded for CPD when compared with PDO fuels at rated load. Since NO_x levels are greatly governed by exhaust gas temperature (EGT), the period of duration for which the exhaust gases remain in cylinder for reduction reaction to accelerate and the abundance of radicals available for NO_x mechanism, the reason for the increase in NO_x emissions with PDO fuel might possibly due to reasons: (1) increase in the overall heat release rate of PDO oil owing to the marginally higher calorific value of PDO oil and subsequent rise of in-cylinder temperature; and (2) higher cetane number, relative to CPD fuel, leading to earlier generation of combustive gases that in turn lead to prolonged remain of exhaust gases for more time in the cylinder. This is also supported by the earlier works (Knothe et al. 2006) that a dependency of higher unsaturated compounds for the increase in NO_x levels. This is also correlating with the composition of compounds in the test fuel under this study that PDO fuel has 15.92% alkenes as against 3.4% in CPD as found in GC-MS analysis. The reason for this, as explained in combustion characteristics, might possibly be because of the double-bonded structure of alkene brakes easily than alkanes paving route for the earlier oxygen radical production for subsequent oxidative combustion reaction which eventually increases the heat release rate and the in-cylinder temperature. Further, the water emulsions of PDO and CPD base fuels showed a reduction of 4.87 and 3.89% in NO_x levels to that of their base fuels. This might be attributed because of the reduction in CV, increase in cetane index which are the indicators for reduction of in-cylinder temperature, and poor combustion efficiency. This is correlating with the reduction in thermal efficiency as discussed in performance characteristics. It also throws light on the fact that participation of water particles during combustion is not fully exploited or not in irradiance to combustion flame.

The variation of $BSNO_x$ with varying bmep for CPD, PDO, and their respective emulsions are shown in Fig. 12. The NO_x levels of PDO 2S 5W $20TiO_2$ was recorded lower than the PDO fuel by 15.5% which might be due to the reduction of in-cylinder temperature consequent to the overall heat release rate during combustion. However, within the PDO with NPs fuel emulsions considered for study, it is observed that the NO_x level increases with the increase in loading ratio of TiO_2 as the amount of encapsulated nanowater particles increases, but this increase is also marginal at low loads and significant after mid load up to rated load. However, the PDO 2S 5W $60TiO_2$ recorded the highest NO_x level of 7.81 g/kWh among the emulsions which is still lower than 7.13% that of PDO fuel under study. This could possibly be due to the following two reasons: (1) the reduction of retention time of exhaust gases at elevated temperature. The increase in temperature of combustion only during in diffused combustion phase has been evidenced from the combustion curve relative to PDO. May be since its net CV is lesser than the PDO, an increase in SFC ought to have increased the heat release rate. However, since the combustion acceleration happened in later period of combustion that too for a shorter CA swipe, approximately for two degrees nearer to TDC as evidenced in combustion data analysis (Table 9), might have reduced the retention time of exhaust gases at elevated temperature for the sufficient reduction reaction to continue in NO_x mechanism. This tradeoff between retention time and HRR might have exerted control over the acquired in-cylinder temperature for not crossing over than that of PDO but higher than its water emulsions. (2) Abundance of radical generation. As explained in the combustion characteristics, the combustion acceleration might be as a result of higher amount of oxygen radicals from the disassociated water molecules. On the other side, the oxygen radicals generated from disassociation of water attacks the nitrogen in supply air and forms nitrogen radical (NO). This nitrogen radical in turn attacks oxygen in air and produces another NO and the reduction reaction continues. Since the retention time is lesser in spite of increased EGT than water-base fuel emulsions without Nps, the disassociated water molecules would not have sufficient time for NO_x to form as the TiO_2 loading rate increases when compared with plain PDO base fuel. However, the increased EGT might have helped in better combustion of hydrocarbon and consequential reduction of CO and HC. Since both the oxidation and reduction reactions

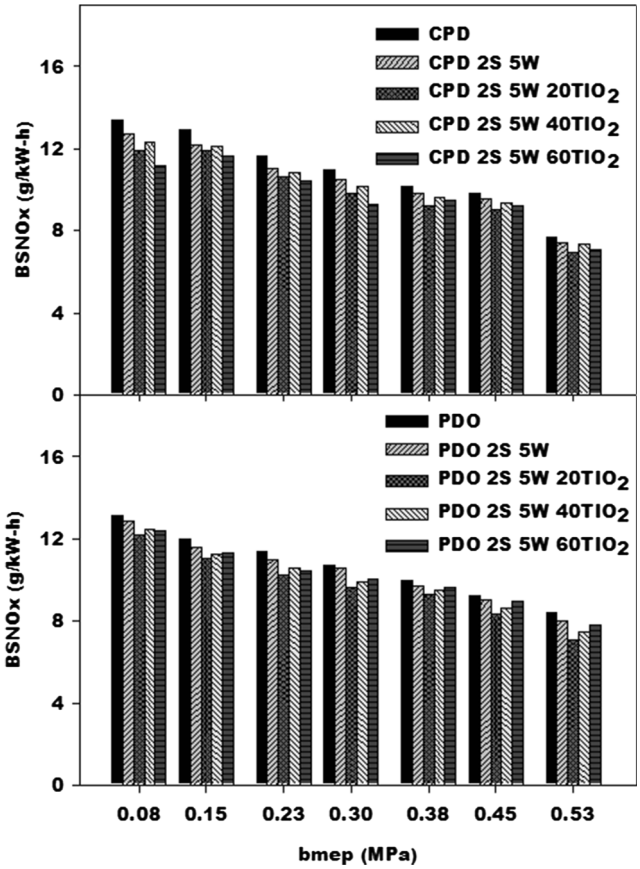

Fig. 12 Variation of $BSNO_x$ with respect to bmep for test fuels

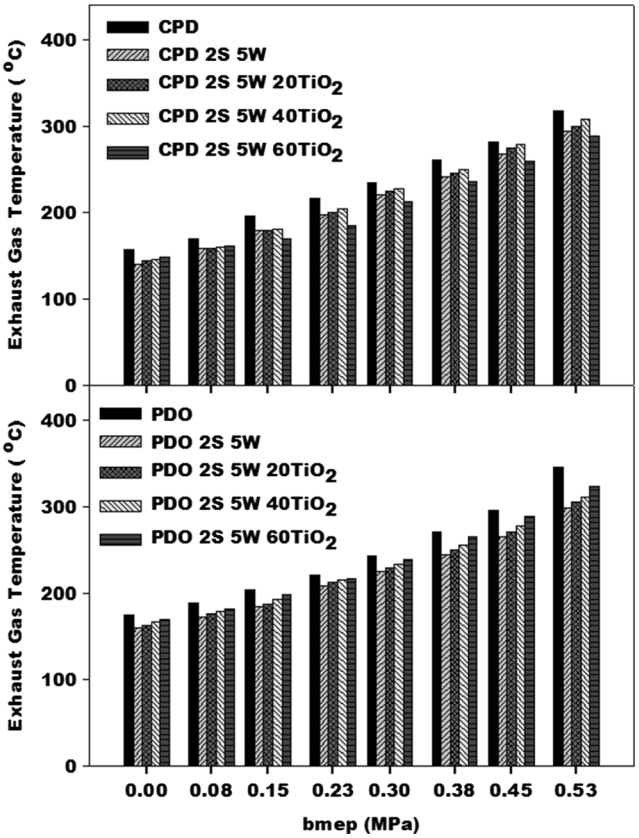

Fig. 13 Variation of EGT with respect to bmep for test fuels

work sequentially in NP emulsion fuel combustion and resulting in increase in peak pressure, NO_x level increases as load and NP loading rate increases when compared with PDO 2S 5W (PDO 2S 5W 60TiO_2 > PDO 2S 5W 40TiO_2 > PDO 2S 5W 20TiO_2). Hence, it is of the opinion that higher loading of water and TiO_2 further is not advisable at least within the range of test fuels under study. The same trend is recorded with CPD and its TiO_2 emulsion fuels. However, the recorded NO_x levels were lesser by 5.88% for CPD 2S 5W 40 than PDO 2S 5W 60 due to the physical and chemical properties of PDO base fuel which were conducible for NO_x formation.

The recorded EGT of the PDO fuel is higher by 7.82% than the CPD at rated load. This is relevant with the earlier discussions that the PDO fuel possessed alkane compounds having higher chemical energy owing to their higher bond strength and molecular compactness in higher percentage than CPD fuel. The EGT of 345.2 °C, maximum among the ten test fuels under study, was recorded during combustion of PDO fuel under study. Figure 13 represents the tendency of change in the EGT of the PDO and CPD test fuels along with their corresponding emulsions. Water emulsions PDO and CPD fuels recorded a reduction of 13.4 and 7.29% in EGT respectively than their base fuels. The EGT decreased for water emulsions of PDO and further an increasing trend was observed for nano-emulsions of relative to PDO. This trend is predominant as the load increases. The reason for the fluctuating trend was already discussed in detail in the NO_x analysis. The same trend prevailed in CPD emulsions except for CPD 2S 5 W 60TiO_2 fuel under study. The resembling catalytic effect was reported by the earlier work (Vellaiyan and Amirthagadeswaran 2016) of water emulsion fuels. A lowest temperature, among water emulsions, of 296 °C was recorded for CPD 2S 5 W fuel. The CPD 2S 5 W 60TiO_2 recorded the lowest of 289.3 °C. This could be due to the unstable dispersion of the colloidal fuel.

Figure 14 illustrates the variation of smoke opacity with bmep for CPD, PDO, and their respective emulsions. An increase of 26.74% in the smoke emission with CPD as fuel against PDO was recorded which could be due to presence of its higher aromatic content (21.1% as against 8.5% in PDO) than that of the PDO fuel under study. The aromatics while combusting produce earlier carbon soot during the premixed combustion phase itself (Millikan 1962). This could be the reason for the relatively increased smoke emissions from the CPD fuel. Further it was observed among PDO emulsion fuels that, a reduction of 8.7, 17.1, 21.3, 26.6% for PDO 2S 5W, PDO 2S 5W 20TiO_2, PDO 2S 5W 40TiO_2, PDO 2S 5W 60TiO_2 respectively in smoke opacity, when compared with the base PDO fuel at rated load. It is also observed that the reduction rate of smoke opacity increases as the load increases due to the catalytic effect as explained in combustion

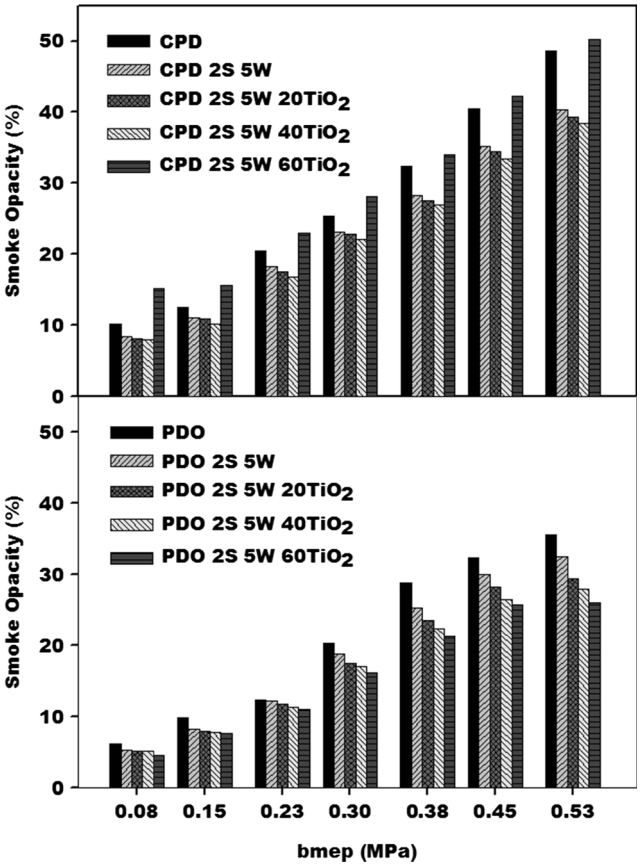

Fig. 14 Variation of smoke opacity with respect to bmep for test fuels

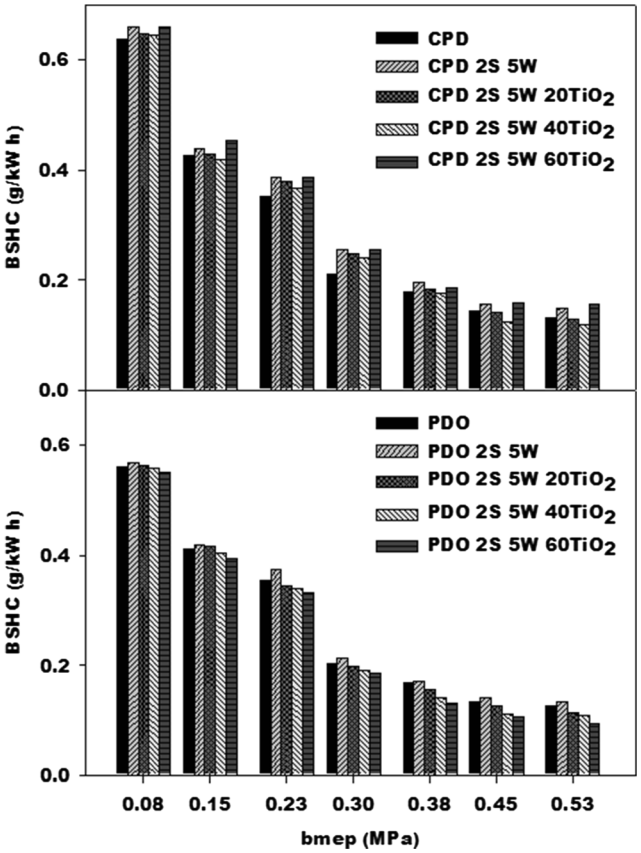

Fig. 15 Variation of BSHC with respect to bmep for test fuels

characteristics and hence the higher temperature produced might have combusted the early formed carbon particles. A reduction of 32.2% in smoke opacity of was recorded during PDO 2S 5 W 60TiO_2 combustion than that of CPD 2S 5 W 40TiO_2 at rated load.

The variation of BSHC with bmep for CPD, PDO, and their respective emulsions are represented in Fig. 15. The BSHC emission of PDO fuel was recorded lower than the CPD fuel by 4.27% at rated load. This might be due to better atomization of fuel for same injection pressure owing to it is relatively lower density and viscosity. High viscosities cause bigger droplet sizes and retard the vapor pressure. Flame extermination in the cold regions of the combustion ambient surrounding inner walls of the cylinder are the prime reasons for HC emissions and are also interrelated with fuel volatility. Correlating the earlier work (Knothe et al. 2006) report that the decrease in chain length of the fuel compounds had a strong effect in reducing BSHC emissions, PDO fuels under study possessing more percentage of lower carbon number range might have contributed to reduction of BSHC emissions. In another research work (Cataluña and da Silva 2012), it was reported that increase in cetane number reduces the HC emissions due to accelerated oxidation of fuel. Since CPD fuel has a reduction of 3.9 units of cetane index than PDO, this could be possible factor for the observed result. An increasing trend in BSHC emissions was recorded for water emulsions of PDO and CPD to a tune of 5.7 and 14.35% respectively than their base fuels. This might be attributed to the increase in viscosity and obviously, lager molecular size of water particles in the emulsion obtained after ultrasonication. Further, the TiO_2 nanoemulsions recorded a decrease in BSHC emissions by 8.6, 13.4, and 16.26% for PDO 2S 5W 20TiO_2, PDO 2S 5W 40TiO_2, and PDO 2S 5W 60TiO_2 respectively and 1.6, 9.5 % for CPD 2S 5W 20TiO_2, CPD 2S 5W 40TiO_2 respectively at rated load than that of their base fuels. However, the decrease showed an accelerated trend as the load increases. This might be due to the overriding effect of combustion optimization during diffused phase over the base fuels against the viscosity component at higher temperatures. Hence, from the emission of BSHC point of view, it is of the opinion that the interaction of oxygen radicals, formed from nanowater particle explosions during diffused combustion phase, with fuel that reacts to combust higher hydrocarbons is beneficial. The BSHC emission of The CPD 2S 5 W 60TiO_2 recorded an increase by 19.23% at rated load against its base fuel. This is possibly be ascribed by the poor stability of the emulsion fuel. Similarly in case of PDO 2S 5 W 60TiO_2, the reduction trend in BSHC emission when compared with PDO 2S 5 W 40TiO_2 is less. Hence, further increase in TiO_2 for both the base fuels may not be helpful within the range of test fuels considered for study.

Carbon monoxide emission could be decreased through early ignition which gives adequate time for combustion in high cetane number fuels (Lilik and Boehman 2011).The CO emission of PDO fuel recorded 18.99% reduction relative to CPD fuel in brake specific basis at rated load. The higher cetane number and distribution of carbon number of compounds present in PDO fuel that are conducive for complete combustion are the reasons for the lesser CO emission. The water emulsions of CPD and PDO fuels recorded an increase of 10.19 and 9.84% respectively than their base fuels. The increase in the BSCO values might be due to poor air fuel mixing due to higher viscosity, delayed combustion due to higher cetane number. Further, PDO 2S 5W 20TiO_2, PDO 2S 5W 40TiO_2, PDO 2S 5W 60TiO_2, CPD 2S 5W 20TiO_2, and CPD 2S 5W 40TiO_2 emulsions fuels recorded 13.05, 19.01, 28.96, 8.96, and 18.91% reduction in CO emissions respectively at rated load than that of their base fuel. This might possibly be because of the higher oxygen radical inclusion owing to the synergic effect of water laden nanoparticles, particularly as load increases, for full combustion. Earlier work (Gumus et al. 2016) also reported the correlation of increased oxygen content during combustion with CO reduction in CI engine. Figure 16 is a comparable depiction of the trend in CO exhaust emissions of CPD and PDO and their emulsion fuels on brake specific basis. CPD 2S 5 W 60 TiO_2 fuel recorded an increase of 10.19% in BSCO emission than that of its base fuel. This could be attributed to the poor emulsion stability which is, obviously, an undesirable characteristic of any fuel.

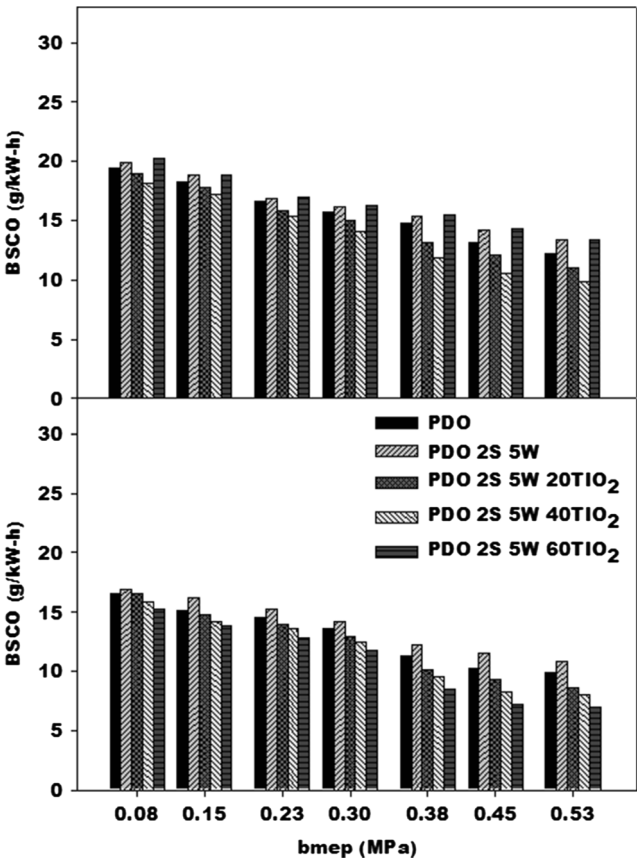

Fig. 16 Variation of BSCO with respect to bmep for test fuels

Conclusion

From the experimentation and characterization studies done on the test fuels, the following salient conclusions have been drawn.

1. The proposed blending technique had shown improvement in the dispersion stability of colloidal nanosuspensions of liquid hydrocarbon-TiO_2-water nano-emulsion for a period of 7 days. This was achieved by the selection and control exercised over the pH of the medium, type of surfactant, dielectric constant of the dispersant and the dispersion medium.

2. Increase in heat release rate (4.12%), EGT (8.55%), and NO_x levels (9.2%) were observed in PDO fuel when compared with the CPD fuel due to the structural influence of higher unsaturated compounds present on PDO fuel (15.92%) as against the CPD fuel (3.4%). This might be due to the weekly bonded double bonded structure resulting in increase in the overall heat release rate and earlier generation of combustive gases leading to prolonged remain of gases for more time in the cylinder.

3. The water emulsions of CPD and PDO fuels showed a decrement in BTE than their base fuels due to the poor exploitation of energy and lower HRR. Reduced calorific value and lower cetane index of water emulsion of PDO fuel as revealed in the characterization studies could be the reason for the rise of BSFC.

4. Water emulsions recorded higher values in ID at low loads and decreases as the load increases but recorded a reduction in BTE, increase in BSHC and BSCO at all loads when compared with nano-emulsions. Insignificant improvement in the HRR, NOx, smoke, was evidenced with PDO-water emulsion fuel which could be due to their poor physical and chemical properties and not had better participation of water particles in diffused phase combustion.

5. TiO_2 emulsions engine experiments revealed that, ignition delay for both CPD 2S 5 W and PDO 2S 5W initially decreases with the addition of TiO_2 nanoparticles (for 20 ppm TiO_2), and then increases with increasing rate of TiO_2 nanoparticles (60 ppm TiO_2). This is due to the synergic effect, i.e. of reduction of 2.5% in cetane index and 6.6% increase in viscosity as observed in the Physico-chemical property evaluation.

6. Improvement in combustion, and emission characteristics of TiO_2 loaded fuels was evidenced due to the combustion acceleration resulting from the secondary explosions of nanosized water droplets loaded over the TiO_2 NPs, at diffused combustion phase. The mechanism behind the improvement of thermal efficiency in spite of the increase in EGT in TiO_2 NPs loaded fuels was due to the overriding effects of increase in peak pressure and reduction of BSFC. The abundance of radical generation and lesser retention period of gases at high temperature in cylinder are the factors responsible for improving the combustion efficiency and reduction of NO_x respectively.

7. In performance characteristics, the recovery of BTE and BSFC was evidenced with TiO_2 particle loaded fuels at higher loads due to the participation of NPs in diffused combustion phase. However, the further increase in loading rates of TiO_2 is not recommended, at least within the scope of test fuels under study, due to the abundance of radical generation and mild increase in combustion noise of the engine. Hence, it is of the opinion that, keeping in mind to strike the balance between the emission and performance characteristics, further research is necessary to tailor made the PDO fuel at pyrolysis stage, during distillation process and before combustion by addition of catalysts, chemical additives, and antioxidants respectively.

Compliance with ethical standards

Conflict of interest The authors declare that they have no conflict of interest.

Nomenclature aTDC, after top dead centre; ASTM, American society for testing and materials; bmep, brake mean effective pressure; bTDC, before top dead centre; BTE, brake thermal efficiency; BSFC, brake specific fuel consumption; BSHC, brake specific hydro carbon; $BSNO_x$, brake specific nitrogen oxides; CA, crank angle; CI, compression ignition; CPD, commercial petro- diesel; CPD 2S 5 W $20TiO_2$, commercial petro- diesel +2% surfactant +5% water +20 ppm titanium dioxide; CPD 2S 5 W $40TiO_2$, commercial petro- diesel +2% surfactant +5% water +40 ppm titanium dioxide; CPD 2S 5 W $60TiO_2$, commercial petro- diesel +2% surfactant +5% water +60 ppm titanium dioxide; CV, calorific value; DLVO, Derjaguin–Landau–Verwey–Overbeek; EGT, exhaust gas temperature; GC-MS, gas chromatography - mass spectrometry; HDPE, high density polyethylene; HLB, hydrophilic–lipophilic balance; HRR, heat release rate; kcps, kilo counts per second; NPs, nanoparticles; PDO, plastic diesel oil; PDO 2S 5 W $20TiO_2$, plastic diesel oil +2% surfactant +5% water +20 ppm titanium dioxide; PDO 2S 5 W $40TiO_2$, plastic diesel oil +2% surfactant +5% water +40 ppm titanium dioxide; PDO 2S 5 W $60TiO_2$, plastic diesel oil +2% surfactant +5% water +60 ppm titanium dioxide; UHC, unburned hydrocarbons

References

Adio SA, Sharifpur M, Meyer JP (2014) Investigation into the pH and electrical conductivity enhancement of MgO - ethylene glycol nano fluids. Proceedings of the 15th International Heat Transfer Conference, https://doi.org/10.1615/IHTC15.tpp.008604

Arianna F, Astorga C, Martini G, Manfredi U, Mueller A, Rey M (2005) Effect of water/fuel emulsions and a cerium-based combustion improver additive on HD and LD diesel exhaust emissions. Environ Sci Technol 39:6792–6799. https://doi.org/10.1021/es048345v

Blocquet M, Schoemaecker C, Amedro D, Herbinet O, Battin-Leclerc F, Fittschen C (2010) Quantification of OH and HO_2 radicals during the low-temperature oxidation of hydrocarbons by Fluorescence Assay by Gas Expansion technique. PNAS 110(50):20014–20017. https://doi.org/10.1073/pnas.1314968110

Brunelli A, Pojana G, Callegaro S, Marcomini A (2013) Agglomeration and sedimentation of titanium dioxide nanoparticles (n-TiO_2) in synthetic and real waters. J Nanopart Res 15(1684). https://doi.org/10.1007/s11051-013-1684-4

Cataluña R, da Silva R (2012) Effect of cetane number on specific fuel consumption and particulate matter and unburned hydrocarbon emissions from diesel engines. J Comb 2012:1–6. https://doi.org/10.1155/2012/738940

Chibowski E, Holysz L, Terpilowski K, Wiacek AE (2007) Influence of ionic surfactants and lecithin on stability of titanium dioxide in aqueous electrolyte solution. Croat Chem Acta 80(3–4):395–403 http://hrcak.srce.hr/18663

Choudhary R, Khurana D, Kumar A, Subudhi S (2017) Stability analysis of Al_2O_3/water nano fluids. Journal of Experimental Nano science 12(1):140–151. https://doi.org/10.1080/17458080.2017.1285445

European Vehicle Market Statistics, (2014) http://www.theicct.org/sites/default/files/publications/ICCT_Pocketbook_2014. Accessed 27 August 2017

Fairhurst D, Lee RW (2011) The zeta potential & its use in pharmaceutical applications—part 1: charged interfaces in polar & non-polar media & the concept of the zeta potential. Drug Development & Delivery 11:6 http://www.particlesciences.com/docs/DDD_July_2011.ZetaPart1.sm. Accessed 16 July 2017

Fowkes FM, Jinnai H, Mostafa M A (1982) Mechanism of electric charging of particles in non aqueous liquids. Colloids and Surfaces in Reprographic Technology, ACS Symposium Series No. 200; Chapter 15: pp 307–324. https://doi.org/10.1021/bk-1982-0200.ch015

Guenther PM, Casavale KO, Kirkpatrick SI, Reedy J, Hiza HAB, Kuczynski KJ, Kahle LL, Krebs-Smith SM (2013) Update of the healthy eating index: HEI-2010. J Acad Nutr Diet 113(4):569–580. https://doi.org/10.1016/j.jand.2012.12.016

Gumus S, Ozcan H, Ozbey M, Topaloglu B (2016) Aluminum oxide and copper oxide nanodiesel fuel properties and usage in a compression ignition engine. Fuel 163:80–87. https://doi.org/10.1016/j.fuel.2015.09.048

Hasannuddin AK, Wira JY, Srithar R, Sarah S, Ahmad MI, Aizam SA, Aiman MAB, Zahari M, Watanabe S, Azrin MA, Mohd SS (2015) Effect of emulsion fuel on engine emissions—a review. Clean Techn Environ Policy. https://doi.org/10.1007/s10098-015-0986-x

Hucknal D J (1985) Chemistry of hydrocarbon combustion. Chapman and Hall Ltd., London, Page 150, ISBN-13: 978-94-010-8649-3. https://doi.org/10.1007/978-94-009-4852-5

Imdadul HK, Masjuki HH, Kalam MA, Zulkifli NWM, Rashed MM, Rashedul HK, Monirul IM, Mosarof MH (2015) A comprehensive review on the assessment of fuel additive effects on combustion behavior in CI engine fuelled with diesel biodiesel blends. RSC Adv 5(83):67541–67567. https://doi.org/10.1039/c5ra09563h

Kaimal VK, Vijayabalan P (2015) A detailed study of combustion characteristics of a DI diesel engine using waste plastic oil and its blends. Energy Convers Manag 105:951–956. https://doi.org/10.1016/j.enconman.2015.08.043

Kalliola S, Repo E, Sillanpää M, Singh Arora J, He J, John VT (2016) The stability of green nanoparticles in increased pH and salinity for applications in oil spill-treatment. Colloids Surf A Physicochem Eng Asp 493:99–107. https://doi.org/10.1016/j.colsurfa.2016.01.011

Kalargaris I, Tian G, Gu S, Kalargaris I, Tian G, Gu S (2017) Combustion, performance and emission analysis of a D.I. diesel engine using plastic pyrolysis oil. Fuel Process Technol 157:108–115. https://doi.org/10.1016/j.fuproc.2016.11.016

Kirby BJ (2009) Micro- and nanoscale fluid mechanics: transport in microfluidic devices. Cambridge University Press, United States of America. http://www.kirbyresearch.com/textbook

Knothe G, Sharp CA, Ryan TW (2006) Exhaust emissions of biodiesel, petrodiesel, neat methyl esters, and alkanes in a new technology engine. Energy Fuel 20(1):403–408. https://doi.org/10.1021/ef0502711

Koo J, Kleinstreuer C (2005) Impact analysis of nanoparticle motion mechanisms on the thermal conductivity of nano fluids. Int Commun Heat Mass Transfer 32(9):1111–1118. https://doi.org/10.1016/j.icheatmasstransfer.2005.05.014

Kumar S, Prakash R, Murugan S, Singh RK (2013) Performance and emission analysis of blends of waste plastic oil obtained by catalytic pyrolysis of waste HDPE with diesel in a CI engine. Energy Convers Manag 74:323–331. https://doi.org/10.1016/j.enconman.2013.05.028

Labib ME, Williams R (1984) The use of zeta potential measurements in organic solvents to determine the donor-acceptor properties of solid surfaces. J Colloid Interface Sci 97(2):356–366. https://doi.org/10.1016/0021-9797(84)90306-0

Lilik GK, Boehman AL (2011) Advanced diesel combustion of a high cetane number fuel with low hydrocarbon and carbon monoxide emissions. Energy Fuel 25(4):1444–1456. https://doi.org/10.1021/ef101653h

Löberg J, Perez Holmberg J, Mattisson I, Arvidsson A, Ahlberg E (2013) Electronic properties of TiO_2 nanoparticles films and the effect on apatite-forming ability. Inte J Dent 2013:1–14. https://doi.org/10.1155/2013/139615

Millikan RC (1962) Nonequilibrium soot formation in premixed flames. J Phys Chem 66(5):794–799. https://doi.org/10.1021/j100811a006

Morrison RT, Boyd RN (1982) Organic chemistry, prentice hall, Dorling Kindersley (India) Pvt. Ltd, INDIA, Section 8.9, Page 319, ISBN-978-81-7758-169-0

Narayanan KS, Anand RB (2016) Experimental investigation on thermocatalytic pyrolysis of HDPE plastic waste and the effects of its liquid yield over the performance, emission, and combustion characteristics of CI engine. Energy Fuel 30(7):5379–5390. https://doi.org/10.1021/acs.energyfuels.6b00407

Sadhik Basha J, Anand RB (2011) An experimental study in a CI engine using nano additive blended water–diesel emulsion fuel. Int J Green Energy 8(3):332–348. https://doi.org/10.1080/15435075.2011.557844

Sadhik Basha J, Anand RB (2014) Performance, emission and combustion characteristics of a diesel engine using carbon nanotubes blended jatropha methyl ester emulsions. Alexandria Engineering Journal 53(2):259–273. https://doi.org/10.1016/j.aej.2014.04.001

Sadhik Basha J (2015) Preparation of water-biodiesel emulsion fuels with CNT & Alumina nano-additives and their impact on the diesel engine operation. SAE Technical Paper 01-0904. https://doi.org/10.4271/2015-01-0904

Samal S, Satpati B, Chaira D (2010) Production and dispersion stability of ultrafine Al–Cu alloy powder in base fluid. J Alloys Compd 504S:S389–S394. https://doi.org/10.1016/j.jallcom.2010.03.223

Selim MYE, Ghannam MT (2007) Performance and engine roughness of a diesel engine running on stabilized water diesel emulsion. SAE Technical Paper 24:132. https://doi.org/10.4271/2007-24-0132

Sen D, Anicich VG, Arakelian T (1992) Dielectric constant of liquid alkanes and hydrocarbon mixtures. J Phys D Appl Phys 25(3):516–521. https://doi.org/10.1088/0022-3727/25/3/027

Shi H, Magaye R, Castranova V, Zhao J (2013) Titanium dioxide nanoparticles: a review of current toxicological data. Part Fibre Toxicol 10(1):15. https://doi.org/10.1186/1743-8977-10-15

Vellaiyan S, Amirthagadeswaran KS (2016) The role of water-in-diesel emulsion and its additives on diesel engine performance and emission levels: a retrospective review. Alexandria Eng J 55(3):2463–2472. https://doi.org/10.1016/j.aej.2016.07.021

Vu P, Nishida O, Fujita H, Harano W (2001) Reduction of NO_x and PM from diesel engines by WPD emulsified fuel. SAE Technical Paper. 01-0152. https://doi.org/10.4271/2001-01-0152

Wang SQ, Zhao Y, Tan Q, Xu PY (2008) Experimental investigation of nano-TiO_2 on combustion and desulfurization catalysis. Huan Jing Ke Xue 29(2):518–524 (in Chinese)

Xian-Ju W, Hai L, Xin-Fang L, Zhou-Fei W, Fang L (2011) Stability of TiO_2 and Al_2O_3 nanofluids. Chin Phys Lett 28(8):086601. https://doi.org/10.1088/0256-307X/28/8/086601

Zawrah MF, Khattab RM, Girgis LG (2016) Stability and electrical conductivity of water-based Al_2O_3 nanofluids for different applications. HBRC J 12(3):227–234. https://doi.org/10.1016/j.hbrcj.2014.12.001